# Scaling, cumulant ratios and height distribution of the ballistic deposition in 3+1 and 4+1 dimensions

Sidiney G. Alves<sup>1,\*</sup> and Silvio C. Ferreira<sup>2,†</sup>

<sup>1</sup>Departamento de Física e Matemática, Universidade Federal de São João Del Rei, 36420-000, Ouro Branco, MG, Brazil

<sup>2</sup>Departamento de Física, Universidade Federal de Viçosa, 36570-000, Viçosa, MG, Brazil

(Dated: July 29, 2021)

We investigate the origin of the scaling corrections in ballistic deposition models in high dimensions using the method proposed by Alves *et al.* [Phys Rev. E **90**, 052405 (20014)] in d=2+1 dimensions, where the intrinsic width associated with the fluctuations of the height increments during the deposition processes is explicitly taken into account. In the present work, we show that this concept holds for d=3+1 and 4+1 dimensions. We have found that growth and roughness exponents and dimensionless cumulant ratios are in agreement with other models, presenting small finite-time corrections to the scaling, that in principle belong to he Kardar-Parisi-Zhang (KPZ) universality class in both d=3+1 and 4+1. Our results constitute a new evidence that the upper critical dimension of the KPZ class, if it exists, is larger than 4.

## PACS numbers: 68.43.Hn, 68.35.Fx, 81.15.Aa, 05.40.-a

## I. INTRODUCTION

Stochastic growth equations play a central role in the understanding of surface growth phenomena and are used to classify the different universality classes [1, 2]. The Kardar-Parisi-Zhang (KPZ) universality class introduced by the stochastic equation [3]

$$\frac{\partial h}{\partial t} = \nu \nabla^2 h + \frac{\lambda}{2} (\nabla h)^2 + \xi, \tag{1}$$

is one of the most fundamental examples of nonequilibrium interface growth model [4–6]. Here,  $h(\mathbf{x},t)$  represents the interface height at the position  $\mathbf{x}$  and time t, the first term in the right-hand side accounts the relaxation due to the surface tension, the second one the local lateral growth in the normal direction along the surface and the last one is a white noise with null mean and amplitude  $\sqrt{D}$ . The benchmark of KPZ class is the lateral growth, second term in Eq. (1), that leads to an excess velocity such that the interface envelop moves faster (or slower if  $\lambda < 0$ ) than the rate at which particles are added in the system.

The interfaces generated by the KPZ equation obey the Family-Vicsek ansatz [7] for the interface width, given by the standard deviation of the height profile, defined as  $w = \sqrt{\langle h^2 \rangle} - \langle h \rangle^2$ . For a scale of observation  $\ell$  and a growth time t, we have that  $w(\ell,t) \sim t^{\beta}$  for  $t \ll \ell^{\alpha/\beta}$  and  $w(\ell,t) \sim \ell^{\alpha}$  for  $t \gg \ell^{\alpha/\beta}$ , where  $\alpha$  and  $\beta$  are the roughness and growth exponents, respectively [1]. The scaling relation  $\alpha + \alpha/\beta = 2$ , representing Galilean invariance, holds independently of the dimension [1]. For 1+1 dimensions the exponents are exactly known as  $\beta = 1/3$  and  $\alpha = 1/2$  [3]; for higher dimensions exponents are obtained from simulations [8–11]. A thorough

analysis of the KPZ class includes the nature of the underlying stochastic fluctuations [5, 6]. Considering the non-stationary regime, the height at each surface point evolves as

$$h = v_{\infty}t + s_{\lambda}(\Gamma t)^{\beta}\chi + \eta + \dots, \tag{2}$$

where  $s_{\lambda} = \operatorname{sgn}(\lambda)$  and  $\chi$  is a stochastic variable, whose distribution is universal and depends on the growth geometries and boundary conditions [12–15]. The constants  $v_{\infty}$  and  $\Gamma$  are non-universal and control, respectively, the asymptotic average velocity and the amplitude of height fluctuations of the interface. The last term in the right-hand side of Eq. (2) is a non-universal correction that plays an important role at finite-time analyses in simulations [16, 17] and experiments [14, 18]. It produces a shift in the distribution of the quantity

$$q = \frac{h - v_{\infty}t}{s_{\lambda}(\Gamma t)^{\beta}},\tag{3}$$

in relation to the asymptotic distribution of  $\chi$ . Except for the very specific case where  $\langle \eta \rangle = 0$  [19], the shift vanishes as  $\langle q \rangle - \langle \chi \rangle \sim t^{-\beta}$  [14, 16–18]. Despite of the absence of exact results in higher dimensions, numerical results show that the KPZ ansatz remains valid up to d=6+1 [9, 17, 20–22].

Discrete growth models are valuable theoretical tools for the realization of universality classes in surface growth phenomena [1, 2] since they permit to flexibly implement specific physical mechanisms. The ballistic deposition (BD) model is a paradigmatic interface growth process initially designed to investigate formation of sediments by the aggregation of small particles from a colloid dispersion [23]. In the BD model, particles move ballistically and normally towards the substrate and are irreversibly attached at the first contact with the deposit, producing, therefore, lateral growth that is a central characteristic of the KPZ universality class [3]. However, the surface evolution exhibits strong corrections in the scaling traditionally attributed to an intrinsic width [24–27] that

<sup>\*</sup> sidiney@ufsj.edu.br

 $<sup>^{\</sup>dagger}$ silviojr@ufv.br

hampers the direct observation of the KPZ critical exponents in this model. Continuous (coarse-grained) limits of the DB model in d = 1 + 1 yield the KPZ equation to leading order but inconsistencies were found in higher dimensions [28, 29]. Preceded by studies lying on finitetime and -size corrections [30, 31] and intrinsic width [24– 27, 32, a direct observation of KPZ universality class for the BD model in d = 1+1 was obtained recently by means of thoroughgoing simulations of very large systems and very long growth times [33, 34]. Recently, a connection between the BD model and the KPZ class in 2+1 dimensions was possible by unveiling the nature of the intrinsic width of the model [22]. It was shown that the leading contribution to the intrinsic width comes from the short wavelength fluctuations in the height increments  $\delta h$  along the deposition events. Besides, it was shown that these effects can be suppressed using a coarse-grained interface built from the original one [22]; see Sec. II.

An important theoretical problem is the upper critical dimension  $d_u$  above which fluctuations become negligible. Analytically, there is no consensus on the value of  $d_u$  (see discussions in Ref. [35]) and an appealing and recent non-perturbative renormalization group analysis rules out  $d_u = 3 + 1$  but the approach losses reliability for  $d \gtrsim 3.5 + 1$  within the approximations considered [36, 37]. Moreover, numerical simulations of models believed as belonging to the KPZ class practically discard  $d_u = 4 + 1$  [8, 35, 38-40] and evidences up  $d_u = 11 + 1$ have been recently reported [9, 10, 41] in agreement with former conjectures [11, 42–44]. While in 2+1 dimensions the generalization of the KPZ ansatz was supported by several models [17, 20, 21], its extension to d > 2 was based on numerical simulations [9] of the restricted-solidon-solid (RSOS) model [45]. In the present work, we investigate the BD model extending the analysis of Ref. [22] to 3+1 and 4+1 dimensions. We verify the validity of the KPZ universality class, including exponents and its ansatz. We also, revisited the values of the cumulants of  $\chi$  presented in Ref. [9] for RSOS model using now more accurate estimates of  $\alpha$ .

The paper is organized as follow. In the next section the model details and the approach used are presented. In section III, the results are presented and discussed. The conclusions are summarized in section IV.

## II. MODEL AND METHODS

The ballistic deposition growth model is implemented in d+1 hypercubic lattices of size L with periodic boundary conditions. The particles are deposited one at a time at a randomly chosen position of a d-dimensional substrate. Each particle is released perpendicularly to the substrate and becomes permanently stuck at the first contact with either the deposit or substrate [1]. The original interface is defined as the highest position of a particle at each site of the substrate. A time unity corresponds to the aggregation of  $L^d$  particles to the deposit.

The simulations were carried out on substrates of sizes up to L=1024 with averages over up to N=2000 independent samples in d=3+1. For d=4+1, we consider systems of size up to L=228 and up to N=1000 samples. The smaller the size the larger the number of samples.

We also investigate surfaces using the prescription of Ref. [22]. The procedure consists in dividing the original surface in bins of lateral size  $\varepsilon$ , the binning parameter, and using only the site of highest height inside each bin to build a coarse-grained interface used to compute statistics. The net effect is that the binned interface is smoother than the original one, the latter characterized by many narrow and deep valleys. In d=2+1, it was shown that the intrinsic width of the coarse-grained surfaces is strongly reduced and, consequently, the strong corrections to the scaling fall off [22]. It was shown that the binning does not change the non-universal constants  $\Gamma$  and  $v_{\infty}$ .

The non-universal constants in the KPZ equation, Eq. (1), and in its ansatz, Eq. (2), can be obtained using the approach hereafter called Krug-Meakin (KM) method [46] that is described as follows. From Eq. (2), the asymptotic velocity is given by

$$\frac{d\langle h\rangle}{dt} = v_{\infty} + \langle g\rangle t^{\beta-1} + \cdots, \tag{4}$$

where  $\langle g \rangle = \beta s_{\lambda} \Gamma^{\beta} \langle \chi \rangle$ . So, plotting  $d\langle h \rangle / dt$  against  $t^{\beta-1}$  renders a straight line for long times with intercept providing  $v_{\infty}$  and the angular coefficient  $\langle g \rangle$ . The latter plays an important role to determine the cumulant ratio  $R = \langle \chi^2 \rangle_c / \langle \chi \rangle^2$ , where  $\langle A^n \rangle_c$  is the notation for nth order cumulant of A; see subsection IIIB. The parameter  $\lambda$  is obtained by the deposition on tilted large substrates with an overall slope s, for which a simple dependence between asymptotic velocity and slope

$$v \simeq v_{\infty} + \frac{\lambda}{2}s^2 \tag{5}$$

is expected for the KPZ equation [46]. We can use the relation [46]

$$\Gamma = |\lambda| A^{1/\alpha},\tag{6}$$

where  $\alpha$  is the roughness exponent of the KPZ class, to determine the amplitude of the fluctuations. The parameter A is obtained from the asymptotic velocity  $v_L$  of finite systems of size L [46] using the relation

$$\Delta v = v_L - v_\infty \simeq -\frac{A\lambda}{2} L^{2\alpha - 2}.$$
 (7)

The KM analysis requires a prior accurate knowledge of the both growth and roughness exponents. In d = 3+1, we adopt the growth exponent  $\beta_{3+1} = 0.184(5)$  reported by Ódor et al. [8] since it has a small uncertainty and was obtained for a model with small corrections to the scaling using large systems of size L = 1024. In d = 4 + 1, we

TABLE I. Non-universal parameter  $\Gamma$  and cumulants of  $\chi$  for RSOS with height restriction parameter m=2 (data from Ref. [9]) obtained using two different values of the roughness exponent reported in the literature for each dimension.

$\overline{d}$	3+1		4+1		
Ref.	Ódor [8]	Marinari [47]	Ódor [8]	Pagnani [35]	
$\alpha$	0.29(1)	0.3135(15)	0.245(5)	0.2537(8)	
$\Gamma$	38(3)	15.8(6)	240(50)	205(8)	
$\langle \chi \rangle$	-0.86	-1.06	-1.00	-1.14	
$\langle \chi^2 \rangle_c$	0.12	0.18	0.09	0.12	

adopt the recent estimate  $\beta_{4+1} = 0.158(6)$  determined by Kim and Kim [38] using a RSOS model with an optimal height restriction parameter that improves the corrections to the scaling. The determination of  $\Gamma$  is extremely sensitive to the value of the roughness exponent since it is used twice in the analysis via Eqs. (6) and (7). In Ref. [9], it was used the exponents of Odor et al. [8], that in d = 4 + 1 is  $\alpha_{4+1} = 0.245(5)$ , and was found for RSOS model  $\Gamma^{(Odor)} = 240(50)$ , that led to  $\langle \chi \rangle_{4+1}^{({\rm Odor})} = -1.00(5)$  and  $\langle \chi^2 \rangle_{{\rm c},4+1}^{({\rm Odor})} = 0.09(1)$  (see Ref. [9] or section IIIB for the procedure to determine these cumulants). Here, we revisit the data of Ref. [9] using a more recent estimate of Pagnani and Parisi [35] given by  $\alpha_{4+1} = 0.2537(8)$  that was obtained doing a thorough finite size analysis and we find a different value  $\Gamma^{(\text{Pagnani})} = 105(8)$  that leads to  $\langle \chi \rangle_{4+1}^{(\text{Pagnani})} = -1.14(2)$ and  $\langle \chi^2 \rangle_{\mathrm{c},4+1}^{\mathrm{(Pagnani)}} = 0.12(1)$  which are, in absolute values, 14% and 30%, respectively, above the estimates of Ref. [9]. Similarly, we revisit the data of Ref. [9] for RSOS in d = 3 + 1 using an former but with smaller uncertainties estimate of  $\alpha_{3+1} = 0.3135(15)$  by Marinari et al. [47], obtained using the same method of Ref. [35], and we find  $\Gamma_{3+1}^{(\mathrm{Marinari})}=15.8(6)$  in contrast with  $\Gamma_{3+1}^{(\mathrm{Odor})}=38(3)$  that was found using  $\alpha_{3+1}=0.29(1)$  [8]. This difference in  $\Gamma$  leads to first and second cumulants approximately 20% and 50% bigger than those found using  $\alpha_{3+1} = 0.29(1)$ . The results are summarized in table I.

## III. RESULTS AND DICUSSIONS

### A. Scaling and intrinsic width

Figure 1(a) shows the interface width evolution in d=3+1 considering the original surface of the BD model as well as those obtained with binning parameters  $\varepsilon=2,\ 4$  and 8. The effective growth exponents, given by the local derivative of  $\ln w$  versus  $\ln t$ , are shown in Figs. 1(b) and (c). As aforementioned, the time evolution of the interface width for the original BD surfaces exhibits strong corrections in the scaling, leading to a very low effective exponent  $\beta_{\rm eff}$ . In particular,  $\beta_{\rm eff}$  becomes close to zero for d=4+1 in the investigated

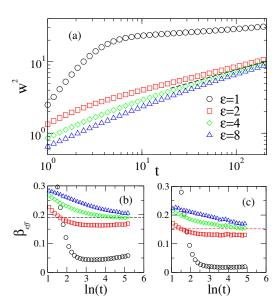


FIG. 1. (a) Time evolution of the squared interface width of the BD model for both original ( $\varepsilon = 1$ ) and reconstructed surfaces in d = 3 + 1. The dashed line is a power law with exponent  $2\beta = 0.368$ . Similar behavior is observed for d = 4 + 1. Effective growth exponents,  $\beta_{\rm eff} = d(\ln w)/d(\ln t)$ , are shown in bottom panels for (b) d = 3 + 1 and (c) 4 + 1. The dashed horizontal lines are the growth exponents found for other models in the KPZ class with small corrections to the scaling in the respective dimensions [8, 38].

time interval, which is consistent with an upper critical dimension  $d_u=4$ . However, as in the previous d=2+1 analysis [22], a convergence to the KPZ growth exponent is observed for the coarse-grained surfaces with  $\varepsilon>1$  in both d=3+1 and 4+1, see Fig. 1. Notice that there is an optimal interval of bin size where the convergence becomes faster. Indeed, if the bin size is very small the reconstructed surface still has narrow and deep valleys and thus a high intrinsic width. On the other hand, if  $\varepsilon$  is too large, only extremal heights are accessed in the statistics and the convergence slows down.

The strong corrections observed in the interface width scaling can be reckoned with an additive term, the squared intrinsic width  $w_i^2$  [25–27, 32], in the Family-Vicsek ansatz [7] as

$$w^{2}(L,t) = L^{2\alpha} f\left(\frac{t}{L^{z}}\right) + w_{i}^{2}, \tag{8}$$

where the scaling function f(x) behaves as  $f(x) \sim x^{2\beta}$  if  $x \ll 1$  and  $f(x) \sim$  constant if  $x \gg 1$ . The intrinsic width can be set in terms of the KPZ ansatz, Eq. (2), as [22]

$$w_i^2 = \langle h^2 \rangle_c - (\Gamma t)^{2\beta} \langle \chi^2 \rangle_c. \tag{9}$$

According to Eq. (2), the second cumulant of the height is given by

$$\langle h^2 \rangle_c = (\Gamma t)^{2\beta} \langle \chi^2 \rangle_c + 2(\Gamma t)^{\beta} \operatorname{cov}(\chi, \eta) + \langle \eta^2 \rangle_c + \dots, (10)$$

where  $\operatorname{cov}(\chi, \eta) = \langle \chi \eta \rangle - \langle \chi \rangle \langle \eta \rangle$ . The cumulant  $\langle g^2 \rangle_c = \Gamma^{2\beta} \langle \chi^2 \rangle_c$  [16], necessary to compute  $w_i$ , can be estimated considering the long time limit of

$$\langle g^2 \rangle_c = \lim_{t \to \infty} \frac{\langle h^2 \rangle_c}{t^{2\beta}}$$
 (11)

Assuming that there is no statistical dependence between  $\chi$  and  $\eta$ ,  $\operatorname{cov}(\chi,\eta)=0$ , a linear extrapolation to  $\langle g^2\rangle_c$  is expected in curves  $\langle h^2\rangle_c/t^{2\beta}$  against  $t^{-2\beta}$ , as confirmed in Fig. 2 in both dimensions for three values of the binning parameter. Propagating the uncertainties in the growth exponents, the estimated values are  $\langle g^2\rangle_c^{(3+1)}=1.4(1)$  and  $\langle g^2\rangle_c^{(4+1)}=0.93(8)$ ; see table II.

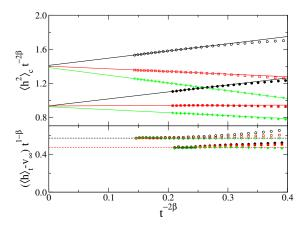


FIG. 2. Determination of nonuniversal cumulants. Top:  $\langle g^2\rangle_c = \Gamma^{2\beta}\langle \chi^2\rangle_c$  for d=3+1 (open symbols) and 4+1 (filled symbols) for DB using binned substrates with  $\varepsilon=2, 4$ , and 8 from top to bottom. The lines are linear regressions used to determine  $\langle g^2\rangle_c$ . Bottom: determination of  $\langle g\rangle = \beta\Gamma\langle\chi\rangle$  for d=3+1 (open symbols) and 4+1 (filled symbols) for DB using binned substrates with  $\varepsilon=2, 3$ , and 4. Dashed lines are estimates of  $\langle g\rangle$ .

The leading contribution to the intrinsic width in d=2+1 comes from the large fluctuations of the height increments in the deep valleys of the BD interfaces [22]:  $w_i^2 \approx \langle (\delta h)^2 \rangle_c$  where  $\delta h(i,t) = h(i,t+dt) - h(i,t)$  is the increment at site i at a step time  $dt = 1/L^d$ . In the present work, we verify that this conjecture is still accurate for d = 3 + 1 and 4 + 1. The upper inset of Fig. 3(a) shows the time evolution of the squared intrinsic width, Eq. (9), and of the second cumulant of  $\delta h$ . We observe a very good accordance between these quantities. The intrinsic widths found for long times, propagating the uncertainties in both  $\beta$  and  $\langle g^2 \rangle_c$ , were  $w_i^{(3+1)} = 21.1(1)$ and  $w_i^{(4+1)} = 32.6(1)$  while for the height increments we found  $\langle (\delta h)^2 \rangle_c = 21.13$  and 32.10 in d = 3 + 1 and 4+1, respectively; see table II. This shows that the corrections in the scaling become more relevant at higher dimensions and explains why it is currently impossible to see KPZ exponents in the high dimensional BD model using a plain analysis. We also compared the third cumulant of  $\delta h$  with  $\langle h^3 \rangle_c - (\Gamma t)^{3\beta} \langle \chi^3 \rangle_c$  and a small but relevant

TABLE II. Non-universal parameters for BD model.

d	$\langle g \rangle$	$\langle g^2 \rangle_c$	$\langle (\delta h)^2 \rangle_c$	$w_i^2$
3+1	0.568(5)	1.40(1)	21.13	21.1(1)
4 + 1	0.466(5)	0.93(8)	31.10	32.6(1)

difference was found, as in d = 2 + 1 [22], showing a non-trivial relation between the height increments and corrections terms in Eq. (2).

The evolution of the interface width discounting  $\langle (\delta h)^2 \rangle_c$  for original BD interfaces is shown in the main panel of the Fig. 3(a). Differently from the binning procedure, this method is free from adjustable parameters. The growth exponents found were  $\beta_{3+1} = 0.185(5)$  and  $\beta_{4+1} = 0.145(10)$ , in sharp agreement with the exponent  $\beta_{3+1} = 0.184(5)$  of Ref. [8] and in marginal agreement with the recent estimate  $\beta_{4+1} = 0.158(6)$  of Ref. [10], as can be seen in the effective exponent analysis in the bottom inset of Fig. 3(a). Here, it is worth to note that the intrinsic width is slightly larger than  $\langle (\delta h)^2 \rangle_c$  in d=4+1, that, together with the finite time used, can explain the slightly smaller growth exponent found in this dimension. This strategy can be used to obtain the roughness exponent  $\alpha$  as well. The squared interface width discounting  $\langle (\delta h)^2 \rangle_c$  is shown as a function of time for different sizes and d = 3 + 1 in Fig. 3(b). The left inset compares the saturated values of  $w^2$  and  $w^2 - \langle (\delta h)^2 \rangle_c$ . We see that the intrinsic width is still much larger than the long wavelength interface width, obtained discounting the intrinsic one, even for the largest investigated size of L = 256. Note that  $\langle (\delta h)^2 \rangle_c$  has as small but not negligible dependence with size that was reckoned in our analysis. The right inset of Fig. 3 shows the effective roughness exponent analysis for d = 3 + 1 and 4+1. The estimated values of roughness exponents are  $\alpha_{3+1} = 0.312(2)$  and  $\alpha_{4+1} = 0.251(5)$  that, withing uncertainties, agree very well with the both estimates  $\alpha_{3+1}^{(\text{Marinari})} = 0.3135(15)$  [47] and  $\alpha_{4+1}^{(\text{Pagnani})} = 0.2537(8)$  [35]. Considering our estimates for the growth exponent we found  $\alpha + \alpha/\beta =$ 2.00(15) and 1.98(15) in d = 3 + 1 and 4+1 dimensions, respectively, in agreement with Galilean invariance scaling relation [3]. In Fig. 3(c), we confirm the validity of the modified Family-Vicsek ansatz, Eq. (8), showing the collapse of  $(w^2 - \langle (\delta h)^2 \rangle_c)/L^{\alpha}$  against  $t/L^{\alpha/\beta}$  in d = 3+1for different systems sizes onto a universal curve.

## B. Height Distribution

Let us now focus on the random variable  $\chi$  of the KPZ ansatz. An initial assessment involves dimensionless cumulant ratios which can be determined without knowing the constants  $\Gamma$  and  $v_{\infty}$ . The skewness S and kurtosis K are given by

$$S = \frac{\langle \chi^3 \rangle_c}{\langle \chi^2 \rangle_c^{1.5}} = \lim_{t \to \infty} \frac{s_\lambda \langle h^3 \rangle_c}{\langle h^2 \rangle_c^{1.5}}$$
 (12)

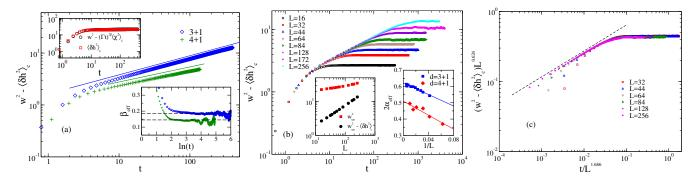


FIG. 3. Interface width analysis for BD in d=3+1 and 4+1. (a) Main panel: squared interface width discounting the second cumulants of height increments for systems of sizes L=1024 and 228 in d=3+1 and 4+1, respectively. The lines are power laws with exponents  $2\beta=0.368$  and 0.290. Top inset: time evolution of the intrinsic width and second cumulant of  $\delta h$  for d=3+1. Bottom inset: effective growth exponent analysis. (b) Main panel: squared interface width discounting the second cumulants of height increments for d=3+1 and different sizes. Left inset: Saturated squared interface width discounting or not the second cumulant of  $\delta h$  against lattice size for d=3+1. Right inset: Effective roughness exponent analysis for d=3+1 and d+1. (c) Squared interface width in d=3+1 scaled with the exponents found in our analysis.

and

$$K = \frac{\langle \chi^4 \rangle_c}{\langle \chi^2 \rangle_c^2} = \lim_{t \to \infty} \frac{\langle h^4 \rangle_c}{\langle h^2 \rangle_c^2},\tag{13}$$

being the right-hand sides obtained with Eq. (2). Another useful cumulant ratio is given by [16, 17]

$$R = \frac{\langle \chi^2 \rangle_c}{\langle \chi \rangle^2} = \frac{\beta^2 \langle g^2 \rangle_c}{\langle g \rangle^2},\tag{14}$$

were  $\langle g \rangle = \beta \Gamma^{\beta} \langle \chi \rangle = \lim_{t \to \infty} (\langle h \rangle_t - v_{\infty}) t^{1-\beta}$ , see Eq. (4) and Fig. 2. The analyses of these cumulant are shown in Fig. 4. We can see that the cumulant ratios are either very close or approaching the values obtained for the RSOS model<sup>1</sup> in Ref. [9], corroborating these KPZ signatures for BD in higher dimensions.

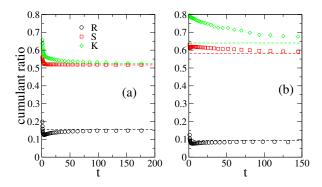


FIG. 4. Determination of dimensionless cumulant ratios for BD in (a) d=3+1 and (b) 4+1. Dashed lines represent the estimates of cumulant ratios for RSOS model taken from Ref. [9]. The BD results were obtained using a binning parameter  $\varepsilon=4$ .

To numerically determine the probability distribution function  $\rho(\chi)$  requires accurate estimates of the non universal constants  $v_{\infty}$  and  $\Gamma$ . The determination of the asymptotic velocities for d=3+1 and 4+1 are shown in the main panel of the Fig. 5. As observed in d=2+1 [22], the asymptotic growth velocity is independent of  $\varepsilon$ , and converges to the same value as the original surface. Our estimated values of the velocity are  $v_{\infty,3+1}=4.49820(2)$  and  $v_{\infty,4+1}=5.60615(5)$ , see table III. Notice that since the asymptotic velocity does not dependent on  $\varepsilon$ , the KM analysis also does not. The determination of  $\lambda$  using Eq. (5), shown in the left inset of Fig. 5, provides  $\lambda_{3+1}=2.81(1)$  and  $\lambda_{4+1}=3.17(4)$ .

The KM curves used to determine the values of  $\lambda A$ , Eq. (7), with the roughness exponents  $\alpha_{4+1}^{(\mathrm{Marinari})} = 0.3135(15)$  and  $\alpha_{4+1}^{(\mathrm{Pagnani})} = 0.2537(8)$ , are shown in the right inset of Fig. 5. The values of  $\Gamma = |\lambda|A^{1/\alpha}$  found are  $\Gamma_{3+1}^{(\mathrm{Marinari})} = 205(20)$  and  $\Gamma_{4+1}^{(\mathrm{Pagnani})} = 730(30)$ . Using our exponents,  $\alpha_{3+1} = 0.312(2)$  and  $\alpha_{4+1} = 0.251(5)$  we have found  $\Gamma_{3+1} = 215(15)$  and  $\Gamma_{4+1} = 700(200)$ . Using the exponent of Ref. [8],  $\alpha_{3+1} = 0.29(1)$  and  $\alpha_{4+1} = 0.245(5)$ , we have found  $\Gamma_{3+1}^{(\mathrm{Odor})} = 500(200)$  and  $\Gamma_{4+1}^{(\mathrm{Odor})} = 1200(250)$ , both presenting large uncertainties and in odds with the previous estimates. In the remaining of the analysis we use  $\Gamma_{3+1} = 205(20)$  and  $\Gamma_{4+1} = 730(30)$  remarking that using the estimates with the exponent of Ref. [8] leads to values consistent with our previous analysis of Ref. [9]. The KM parameters are summarized in Table III.

Possessing the KM parameters, the first and second cumulants of  $\chi$  can be obtained directly from

$$\langle \chi \rangle = \frac{\langle g \rangle}{\beta \Gamma^{\beta}} \tag{15}$$

and

$$\langle \chi^2 \rangle_c = \frac{\langle g^2 \rangle_c}{\Gamma^{2\beta}},$$
 (16)

 $<sup>^1</sup>$  Differently from the cumulants of  $\chi$  (see section II), the cumulant ratios obtained for RSOS model in Ref. [9] are reliable references because the model has small finite-time corrections and the determination does not depend on  $\alpha.$ 

TABLE III. Non-universal KM parameters and cumulants of  $\chi$  for DB model.

d	$v_{\infty}$	λ	Γ	$\langle \chi \rangle$	$\langle \chi^2 \rangle_c$
3+1	4.49820(2)	2.81(1)	205(20)	-1.15(3)	0.197(7)
4 + 1	5.60615(5)	3.17(4)	730(30)	-1.04(1)	0.115(3)

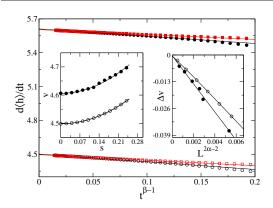


FIG. 5. Parameter determination using KM method [46]. Main panel: Interface growth velocity for BD in d=3+1 (bottom curves) and 4+1 (top curves) are represented by open and filled symbols, respectively. We show the results for the original surface (squares) and binning parameter  $\varepsilon=4$  (circles). Left Inset: growth velocity against substrate slope for d=3+1 (open symbol) and 4+1 (filled symbols). The velocity in d=4+1 is subtracted by 1 to improve visualization. Right inset: linear dependence of the velocity difference  $\Delta v=v_L-v_\infty$  with the system size according Eq. (7).

where  $\langle g \rangle$  and  $\langle g^2 \rangle_c$  are defined in Sec. II and shown in table III. The results are  $\langle \chi \rangle_{3+1} = 1.15(3)$ ,  $\langle \chi \rangle_{4+1} = 1.04(1)$ ,  $\langle \chi^2 \rangle_{c,3+1} = 0.197(7)$  and  $\langle \chi^2 \rangle_{c,4+1} = 0.115(3)$ , which are in very good agreement with the corresponding cumulants for RSOS shown in table II. These cumulants are summarized in table III.

Lets us define the random variable

$$q' = \frac{h - v_{\infty}t - \langle \eta \rangle}{(\Gamma t)^{\beta}} \tag{17}$$

whose probability distribution function converges to  $\rho(\chi)$  as  $t \to \infty$  [16, 17]. To determine the parameter  $\langle \eta \rangle$  we use that

$$\frac{\langle h \rangle - v_{\infty} t}{t^{\beta}} = \Gamma^{\beta} \langle \chi \rangle + \langle \eta \rangle t^{-\beta} + \cdots, \qquad (18)$$

such that plotting this left-hand quantity against  $t^{-\beta}$  extrapolates linearly to  $\Gamma^{\beta}\langle\chi\rangle$  and the angular coefficient is  $\langle\eta\rangle$ . Figure 6 confirms the expected behavior and the existence of the correction. Since  $\eta$  is a short wavelength correction, the value of  $\langle\eta\rangle$  depends on the binning parameter  $\varepsilon$  [22], as shown in table IV.

In Fig. 7, the probability distribution functions for binned surfaces in d = 3 + 1 and 4+1 are compared with those of the original interface as well as with those of RSOS model, the last one built using the estimates of  $\Gamma$ 

TABLE IV. Average value of the correction  $\eta$  in the KPZ ansatz, Eq. (2) and Fig. 6.

$\overline{d}$	$\epsilon = 1$	$\epsilon=2$	$\epsilon = 4$	$\epsilon = 8$
3+1	-2.3	1.9	3.9	5.7
4+1	-3.9	1.9	4.1	6.1

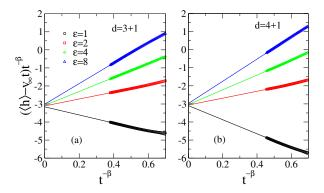


FIG. 6. Determination of the average shift  $\langle \eta \rangle$  in (a) d=3+1 and (b) 4+1.

of table I while the other parameters are those reported in Ref. [9]. If, on the one hand, the original surfaces are not close to the RSOS distributions, on the other hand, we see a satisfactory agreement with the binned surfaces, presenting small deviations in either left or right tails for d=3+1 and 4+1, respectively. These deviations must shrink if much longer growth times are considered.

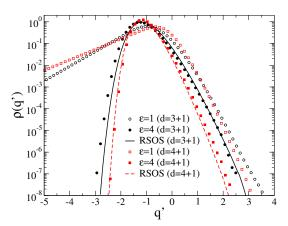


FIG. 7. Comparison of the probability distribution function, Eq. (17), of the original and binned surfaces of the BD model in d = 3 + 1 and 4+1 dimensions with the RSOS model. The growth times in BD models are t = 190 and 145 for d = 3 + 1 and 4+1, respectively.

### IV. CONCLUSIONS

Ballistic deposition growth models are characterized by a prominent lateral growth and therefore are considered standards of KPZ growth [1]. However, strong finite-time and -size corrections make a direct realization of the KPZ exponents in higher dimensions extremely hard and, in practice, unaccessible with our current computer resources. However, eliciting the origin of the leading contributions to the corrections as being due to the fluctuations of height increments along the deposition of particles, it was possible to do a connection between ballistic deposition and KPZ universality class in d=2+1 dimensions [22]. Moreover, using the coarse-grained surface where only the highest points inside small bins of size  $\epsilon \ll \xi$ , where  $\xi$  is the surface correlation length, it was possible to obtain the KPZ exponents as well as the universal underlying stochastic fluctuations of the KPZ class in d=2+1 [22].

In the present work, we show that the methodology of Ref. [22] remains valid for ballistic deposition in d=3+1 and 4+1 dimensions. We observe that the squared intrinsic width is given by  $w_i^2 \approx \langle (\delta h) \rangle_c$ , where  $\delta h$  is the height increment in a deposition step, and becomes more relevant at higher dimensions. Growth and roughness exponents in very good agreement with those reported for KPZ models with small corrections to the

scaling [8, 9, 11, 35, 38] were obtained when the intrinsic width was explicitly reckoned in the scaling analysis. Using a binned surface analysis, we also provide evidences that the underlying fluctuation  $\chi$  of height profiles belongs to the KPZ class, using the dimensionless cumulant ratios and the probability distribution function itself.

We also revisit the data for RSOS deposition model reported in Ref. [9] considering more accurate estimates of the roughness exponents. We have found that the non-universal parameter  $\Gamma$ , representing the amplitude of the interface fluctuations, changes significantly implying in changes of the estimates of the cumulants of  $\chi$ .

Finally, it is worth noticing that our results provide a new numerical evidence for an upper critical dimension, if it exists, larger than d = 4+1 corroborating former [11, 42–44] and recent [9, 10, 35, 41] findings.

### ACKNOWLEDGMENTS

Authors acknowledge the support from CNPq and FAPEMIG (Brazilian agencies).

- [1] A.-L. Barabasi and H. E. Stanley, *Fractal Concepts* in *Surface Growth* (Cambridge University Press, Cambridge, England, 1995).
- [2] P. Meakin, Fractals, Scaling and Growth far from Equilibrium (Cambridge University Press, Cambridge, England, 1998).
- [3] M. Kardar, G. Parisi, and Y.-C. Zhang, "Dynamic scaling of growing interfaces," Phys. Rev. Lett. 56, 889 (1986).
- [4] T. Kriecherbauer and J. Krug, "A pedestrian's view on interacting particle systems, KPZ universality and random matrices," J. Phys. A: Math. Theor. 43, 403001 (2010).
- [5] T. Sasamoto and H. Spohn, "The 1 + 1-dimensional Kardar-Parisi-Zhang equation and its universality class,"
   J. Stat. Mech.: Theor. Exp. 2010, P11013 (2010).
- [6] K. A. Takeuchi and M. Sano, "Evidence for geometrydependent universal fluctuations of the Kardar-Parisi-Zhang interfaces in liquid-crystal turbulence," J. Stat. Physics 147, 853 (2012).
- [7] F. Family and T. Vicsek, "Scaling of the active zone in the Eden process on percolation networks and the ballistic deposition model," J. Phys. A: Math. Gen. 18, L75 (1985).
- [8] G. Ódor, B. Liedke, and K.-H. Heinig, "Directed d-mer diffusion describing the Kardar-Parisi-Zhang-type surface growth," Phys. Rev. E 81, 031112 (2010).
- [9] S. G. Alves, T. J. Oliveira, and S. C. Ferreira, "Universality of fluctuations in the Kardar-Parisi-Zhang class in high dimensions and its upper critical dimension," Phys. Rev. E 90, 020103(R) (2014).
- [10] S.-W. Kim and J. Kim, "A restricted solid-on-solid model in higher dimensions," J. Stat. Mech.: Theor. Exp. 2014, P07005 (2014).

- [11] E. Marinari, a. Pagnani, G. Parisi, and Z. Rácz, "Width distributions and the upper critical dimension of Kardar-Parisi-Zhang interfaces," Physical Review E 65, 026136 (2002).
- [12] J. Krug, P. Meakin, and T. Halpin-Healy, "Amplitude universality for driven interfaces and directed polymers in random media," Phys. Rev. A 45, 638 (1992).
- [13] M. Prähofer and H. Spohn, "Universal distributions for growth processes in 1+1 dimensions and random matrices," Phys. Rev. Lett. **84**, 4882 (2000).
- [14] K. A. Takeuchi, M. Sano, T. Sasamoto, and H. Spohn, "Growing interfaces uncover universal fluctuations behind scale invariance," Sci. Rep. 1, 34 (2011).
- [15] I. S. S. Carrasco, K. a. Takeuchi, S. C. Ferreira, and T. J. Oliveira, "Interface fluctuations for deposition on enlarging flat substrates," New J. Phys. 16, 123057 (2014).
- [16] S. G. Alves, T. J. Oliveira, and S. C. Ferreira, "Non-universal parameters, corrections and universality in Kardar-Parisi-Zhang growth," J. Stat. Mech. 2013, P05007 (2013).
- [17] T. J. Oliveira, S. G. Alves, and S. C. Ferreira, "Kardar-Parisi-Zhang universality class in (2+1) dimensions: Universal geometry-dependent distributions and finite-time corrections," Phys. Rev. E 87, 040102(R) (2013).
- [18] K. A. Takeuchi and M. Sano, "Universal fluctuations of growing interfaces: Evidence in turbulent liquid crystals," Phys. Rev. Lett. **104**, 230601 (2010).
- [19] P. Ferrari and R. Frings, "Finite time corrections in KPZ growth models," J. Stat. Phys. 144, 1 (2011).
- [20] T. Halpin-Healy, "(2+1)-dimensional directed polymer in a random medium: Scaling phenomena and universal distributions," Phys. Rev. Lett. 109, 170602 (2012).
- [21] T. Halpin-Healy, "Extremal paths, the stochastic heat equation, and the three-dimensional kardar-parisi-zhang

- universality class," Phys. Rev. E 88, 042118 (2013).
- [22] S. G. Alves, T. J. Oliveira, and S. C. Ferreira, "Origins of scaling corrections in ballistic growth models," Phys. Rev. E 90, 052405 (2014).
- [23] M. J. Vold, "A numerical approach to the problem of sediment volume," Journal of Colloid Science 14, 168 (1959).
- [24] J. Kertész and D. E. Wolf, "Noise reduction in Eden models: II. surface structure and intrinsic width," J. Phys. A: Math. Gen. 21, 747 (1988).
- [25] E. Moro, "Internal fluctuations effects on fisher waves," Phys. Rev. Lett. 87, 238303 (2001).
- [26] M. Tammaro and J. W. Evans, "Chemical diffusivity and wave propagation in surface reactions: Lattice-gas model mimicking co-oxidation with high co-mobility," J. Chem. Phys. 108, 762 (1998).
- [27] F. Chávez, L. Vicente, A. Perera, and M. Moreau, "Dynamics of front propagation in the catalytic co oxidation on pt(100)," J. Chem. Phys. 110, 8119 (1999).
- [28] E. Katzav and M. Schwartz, "What is the connection between ballistic deposition and the Kardar-Parisi-Zhang equation?" Phys. Rev. E 70, 061608 (2004).
- [29] C. A. Haselwandter and D. D. Vvedensky, "Scaling of ballistic deposition from a Langevin equation," Phys. Rev. E 73, 040101 (2006).
- [30] F. D. A. Aarão Reis, "Universality and corrections to scaling in the ballistic deposition model," Phys. Rev. E 63, 056116 (2001).
- [31] F. D. A. Aarão Reis, "Roughness fluctuations, roughness exponents and the universality class of ballistic deposition," Physica A **364**, 190 (2006).
- [32] T. J. Oliveira and F. D. A. Aarão Reis, "Finite-size effects in roughness distribution scaling," Phys. Rev. E 76, 061601 (2007).
- [33] B. Farnudi and D. D. Vvedensky, "Large-scale simulations of ballistic deposition: The approach to asymptotic scaling," Phys. Rev. E 83, 020103 (2011).
- [34] B. Farnudi and D. D. Vvedensky, "Large-scale simulations with distributed computing: Asymptotic scaling of ballistic deposition," J. Phys.: Conf. Ser. 286, 012031 (2011).
- [35] A. Pagnani and G. Parisi, "Multisurface coding simula-

- tions of the restricted solid-on-solid model in four dimensions," Phys. Rev. E 87, 010102 (2013).
- [36] L. Canet, H. Chaté, B. Delamotte, and N. Wschebor, "Nonperturbative renormalization group for the Kardar-Parisi-Zhang equation," Phys. Rev. Lett. 104, 150601 (2010).
- [37] T. Kloss, L. Canet, and N. Wschebor, "Nonperturbative renormalization group for the stationary Kardar-Parisi-Zhang equation: Scaling functions and amplitude ratios in 1+1, 2+1, and 3+1 dimensions," Phys. Rev. E. 86, 051124 (2012).
- [38] J. M. Kim and S.-W. Kim, "Restricted solid-on-solid model with a proper restriction parameter n in 4+1 dimensions," Phys. Rev. E **88**, 034102 (2013).
- [39] M. Schwartz and E. Perlsman, "Upper critical dimension of the Kardar-Parisi-Zhang equation." Phys. Rev. E 85, 050103 (2012).
- [40] E. Perlsman and S. Havlin, "Optimal paths as correlated random walks," Europhysics Letters (EPL) 73, 178 (2006).
- [41] E. A. Rodrigues, B. A. Mello, and F. A. Oliveira, "Growth exponents of the etching model in high dimensions," J. Phys. A: Math. Theor. 48, 035001 (2015).
- [42] Y. Tu, "Absence of Finite Upper Critical Dimension in the Spherical Kardar-Parisi-Zhang Model," Physical Review Letters 73, 3109 (1994).
- [43] T. Ala-Nissila, T. Hjelt, J. M. Kosterlitz, and O. Venäläinen, "Scaling exponents for kinetic roughening in higher dimensions," J. Stat. Phys. 72, 207 (1993).
- [44] T. Ala-Nissila, "Comment on "Upper Critical Dimension of the Kardar-Parisi-Zhang Equation"," Physical Review Letters 80, 887 (1998).
- [45] J. M. Kim and J. M. Kosterlitz, "Growth in a restricted solid-on-solid model," Phys. Rev. Lett. 62, 2289 (1989).
- [46] J. Krug and P. Meakin, "Universal finite-size effects in the rate of growth processes," J. Phys. A: Math. Gen. 23, L987 (1990).
- [47] E. Marinari, A. Pagnani, and G. Parisi, "Critical exponents of the KPZ equation via multi-surface coding numerical simulations," J. Phys. A: Math. Gen. 33, 8181 (2000).